Optimization of a High Efficiency Civil Tiltrotor platform for Low Emission Flight

Manas Khurana
manas.s.khurana@nasa.gov
Science and Technology Corporation
Moffett Field, CA

Christopher Silva
christopher.silva@nasa.gov
NASA Ames Research Center
Moffett Field, CA

ABSTRACT

Conceptual design of a high efficiency civil tiltrotor (HECTR) as part of NASAs Revolutionary Vertical Lift Technology (RVLT) project is studied using the NASA Design and Analysis of Rotorcraft (NDARC) software with Rotorcraft Optimization Tools (RCOTOOLS) and the particle swarm optimization (PSO) algorithm. A gradient-based method is first applied for rotor disk and wing loading sizing optimization to collectively minimize platform empty, mission fuel weight and engine power requirements. An optimum design from the study is then used to further minimize emissions as a function of cruise altitude. The results confirmed that gradient-based methods are limited as a multimodal solution space exists with local minima's, hence gradient-free methods are required. As pre-processing to an evolutionary search process with PSO, a design variable sensitivity analysis was undertaken to identify the importance of sizing parameters on emissions. The solution generated by the swarm method resulted in significant improvements in emissions relative to baseline and gradient-based methods. The findings confirmed the merits of population-based optimization algorithms for rotorcraft conceptual sizing.

INTRODUCTION

The environmental impact of commercial aviation is of significant importance to the aerospace community and with climate change concerns, the design of aircraft with low emissions and noise becomes a critical design requirement. Accordingly environmental considerations need to be factored at early stages of aircraft design so that a systematic investigation and quantification into the trade-offs involved in meeting specific noise and emissions constraints can be evaluated. It has been shown that improving environmental performance of an aircraft inadvertently results in higher operating costs and/or reduced performance (Ref. 1). In this framework, aircraft design for reduced environmental impact is well suited towards finding an optimal set of solutions using a multi-objective optimization framework. This will allow system level trades between the objectives to be analyzed before a final design is selected.

The development of computational tools and methods to support rotorcraft conceptual and preliminary design by automation using mixed fidelity-solvers in an optimization framework is critical to the study-of-domain. Johnson (Ref. 2) developed NDARC which is a conceptual/preliminary design and analysis code for rapidly sizing and conducting performance analysis of new rotorcraft concepts. Meyn (Ref. 3) introduced RCOTOOLS to couple NDARC with OpenMDAO (Ref. 4) using validated software methods and approaches to facilitate a robust optimization framework. Johnson and Sinsay (Ref. 5) developed an information manager that effectively organizes and shares aircraft data between solvers to facilitate multi-fidelity analysis in a collaborative design environment. Lier et al. (Ref. 6), further developed a conceptual and preliminary design toolbox that models platform geometry in a CAD environment to evaluate the aerodynamic, mass and structural properties of emerging rotorcraft configurations. Enconniere, Ortiz-Carretero and Pachidis (Ref. 7), proposed a multidisciplinary methodology to evaluate the environmental and operational benefits of a compound coaxial rotorcraft. The effects of cruise speed, altitude, climb rate and mission length were evaluated for a mission ranging from 50 to 300 km. Optimization resulted in collective reduction in mission duration, fuel burn, and NO_x (Nitrogen Oxides) emissions. Ali, Goulos and Pachidis (Ref. 8), also presented an integrated multidisciplinary simulation framework that was deployed for the comprehensive assessment of combined helicopter-powerplant system at a mission level to enhance operational performance and to limit environmental impact. Their results suggest that while a helicopter can offer significant improvement in the payload-range capability while simultaneously maintaining the required airworthiness requirements, there is a detrimental impact on emissions, specifically with NO_x. Accordingly this conflicting performance imposes a design trade-off between fuel economy and environmental performance. Similarly Russel and

Presented at the AHS Aeromechanics Design for Transformative Vertical Flight forum, San Francisco, California, USA, January 16–19, 2018.

Basset (Ref. 9), also used computational tools to show that designing rotorcraft for reduced environmental impact significantly influences aircraft configuration as the rotorcraft that would typically operate at high altitudes, is then required to cruise lower and slower to reduce the effect of NO_x which inadvertently increases fuel burn and CO_2 emissions.

The development of computational tools for rotorcraft conceptual design with low environmental impact is a goal. A well-defined concept at conceptual phase will support ongoing performance gains as the design progresses to preliminary and detail design stages. In this work, optimization methods are used to support rotorcraft sizing to minimize emissions for an outlined mission . The software package RCOTOOLS (Ref. 3) with OpenMDAO (Ref. 4), is coupled to NDARC (Ref. 2) to compute platform performances of the entered inputs. The computational framework is also used to explore the topology of the design space as a function of sizing parameters to determine the feasibility of gradient-based optimization methods. In the process, first order design and objective measure sensitivities are evaluated to model the relationship between input parameters on performance output. The optimization framework is also extended with increased dimensionality by the integration of additional sizing parameters in a gradient-free optimization environment to sustain further improvements in emissions.

BACKGROUND

The research undertaken contributes to the state-of-the-art in rotorcraft parametric sizing with focus on the: **(a)** utilization of dedicated software packages developed at NASA to support the design of next generation rotary wing platforms for civil applications; including **(b)** the definition of best-practices and approaches required to support a parametric sizing framework; and **(c)** execution of a parametric sizing process using different configurations of a tiltrotor platform to demonstrate the first-order design sensitivities of the sizing parameters on emissions. The research is to demonstrate the importance of conceptual sizing to ensure the platform can efficiently sustain required mission goals and that the integrated technologies can meet current aerospace demands and challenges. Proper sizing at early design stages will avoid the situation of optimizing a poor concept at later phases.

Engineering optimization problems are represented by a complex solution space that may have many local minima to the objective function with respect to the selected design variables and constraints. Hence, convergence to a single global best solution is not always achievable. Accordingly if multiple solutions (locally and/or globally optimal) are established, they can be analyzed to evaluate the hidden properties (or relationships) between the modeled parameters, and to form problem domain knowledge. Gradient-based optimization algorithms are well suited to transit to a solution from an initial starting point with rapid computation turn-over time relative to population-based algorithms. The knowledge gained from this process, with the formulation of solution landscape topology type (uni-modal or multi-modal) will address if stochastic optimization methods are required to sustain global performance improvements.

In this work, a multi-disciplinary design, analysis and optimization (MDAO) framework is initially used for rotorcraft sizing. This includes a Python-based framework that is applied for a design trade study using the baseline HECTR configuration developed by Silva et al. (Ref. 10). A design sweep is undertaken to qualitatively model the solution topology with input parameters including rotor wing and disk loadings on mission fuel, W_{fuel}, platform empty weight, W_{empty}, and engine power requirements, P_{req}, as a function of cruise altitude. From the database, a candidate solution with an acceptable compromise between the conflicting objectives is selected for further sizing optimization to minimize the Emission Trading Scheme (ETS). The analysis will outline the role of gradient-based methods in conceptual sizing and the limitations of this approach for sizing efforts where problem dimensionality is high.

The analysis will also be extended with a greater degree-of-freedom as additional sizing parameters are introduced. Accordingly evolutionary algorithms will be applied in an effort to further lower emissions by an order of magnitude. The PSO theory (Ref. 11) will be used that is capable of converging to a global minima for complex engineering problems (Refs. 12–19). As population-based algorithms are computationally extensive, a design variable sensitivity analysis will support the study goals to model the impact of sizing parameters on output objective so that unimportant parameters can be identified and excluded from PSO simulations to limit computational overheads. As data post-processing, the success of the gradient-free method in converging to a global minima is examined.

The mission profile that will be used for sizing optimization is presented in Table 1. It represents a civil tiltrotor (CTR) with a high wing configuration and engines in tilting nacelles that are sized to efficiently transport 4-6 passengers. The design mission's first segment is taxi at maximum continuous power for five minutes to burn a representative amount of fuel. The weight at the beginning of the first segment defines design gross weight. The second segment is a hover out of ground effect for five minutes. All hovers are performed with the hover trim state. The third segment is a climb maneuver at 300 ft / minute from take-off to cruise altitude with intermediate rated power. The horizontal distance covered during climb contributes to the total cruise range of 400 nm in segment 4. Segment 5 represents reserve with a flying time of 30 minutes.

Table 1. HECTR Mission Profile Segment Details

Mission Segment	Segment Type	Altitude (ft)	Day	Time (mins)	Distance (nm)	Airspeed (Vkts)[†]	Power Available (%)	Engine Rating
1	taxi/warm-up	5,000	ISA+20°C	5	···	···	100	MCP[a]
2	Hover OGE	5,000	ISA+20°C	5	···	···	95	MRP[b]
3	Climb[d]	5,000	ISA+20°C	···	Credit to cruise	100	95	IRP[c]
4	Cruise	25,000[e]	ISA	···	400 - credit from climb	240	90	MCP
5	Reserve	···	ISA	30	···	150	100	MCP

[a] Maximum Continuous Power; [b] Maximum Rated Power; [c] Intermediate Rated Power
[d] Climb at a rate of climb (ROC) of 300 ft/min from present altitude to next segment altitude
[†] Horizontal velocity (TAS)
[e] Baseline platform cruising altitude at 25,000ft; subject to change with optimization for low emission.

APPROACH

Optimization is defined using the following notation:

$$\begin{aligned} \min \quad & f(x,p) \\ \text{subject to} \quad & g(x,p) \geq 0 \\ & h(x,p) = 0 \end{aligned} \tag{1}$$

$$x_{i,LB} \leq x_i \leq x_{i,UB} (i = 1, \ldots, n)$$

where the objective function vector, $\boldsymbol{f}$, is a function to be minimized (or maximized) over design vector, $\boldsymbol{x}$, and a fixed parameter vector, $\boldsymbol{p}$; $\boldsymbol{g}$ and $\boldsymbol{h}$ are inequality and equality constraints; and $x_{i,LB}$ and $x_{i,UB}$ are the lower and upper bounds for the i_{th} design variable, respectively.

To minimize multiple objectives for the input design vector, a weighted sum approach is used. The objective is transformed into an aggregated function by multiplying each objective by a weighting factor and summing up all weighted objective functions:

$$f_{\text{weighted sum}} = w_1 f_1 + w_2 f_2 + \ldots + w_m f_m \tag{2}$$

where $w_i (i = 1, \ldots, m)$ is a weighting factor for the i_{th} objective function and is selected in proportion to the relative importance of the objective.

Equation 1 is defined in RCOTOOLS with input variables and constraints. The summation of the objectives with weights in Equation 2 is then used by the optimizer for function minimization. Figure 1 outlines the five modules that define the scope of the sizing simulations.

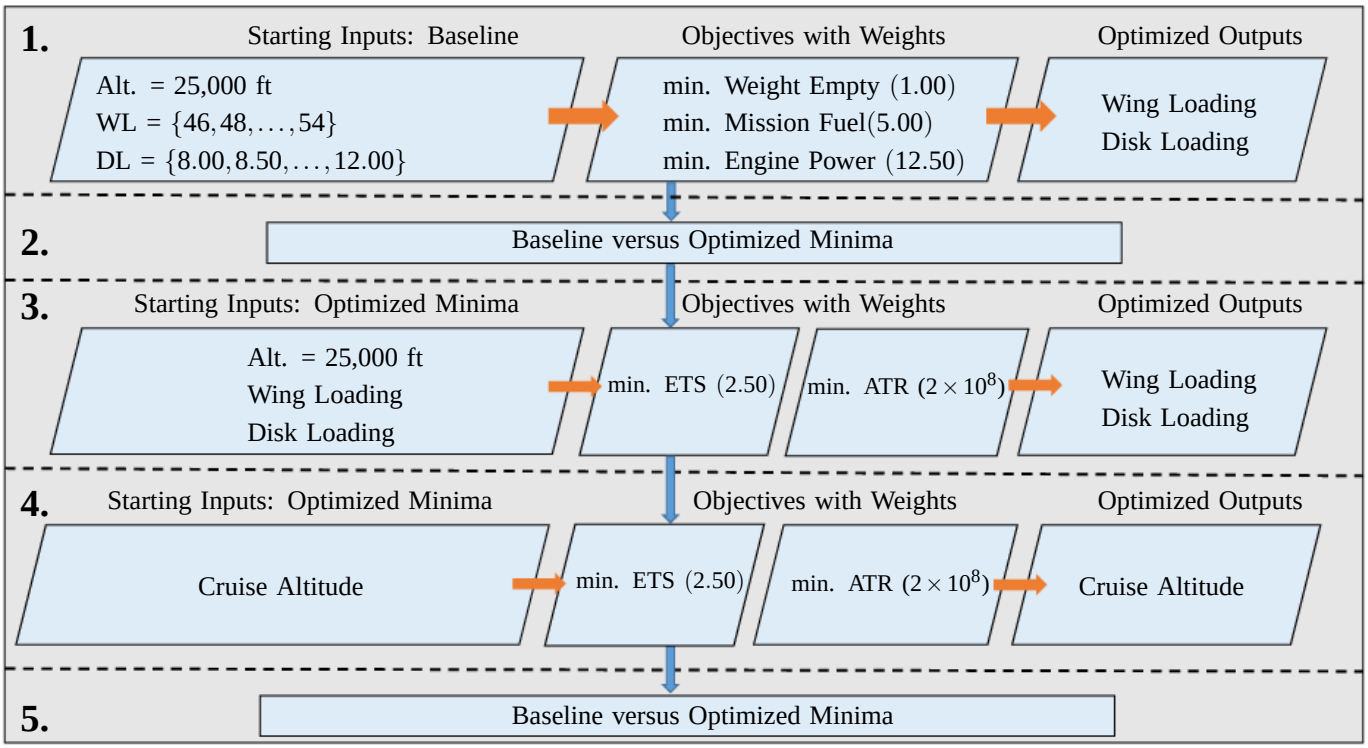

Fig. 1. Overview of the optimization approach used to size HECTR

The gradient-based optimization framework is structured as follows:

1. A parametric sweep is executed that varies the wing and disk loading of the baseline (Ref. 10) over a defined interval range at fixed cruise altitude. A weighted sum method is imposed to define the multi-objective fitness function that minimizes platform W_{empty}; W_{fuel}; and P_{req}. The outputs will represent the optimized configuration of wing and disk loading.
2. A configuration with low W_{fuel} from the database in module one is identified and compared to baseline (Ref. 10).
3. The selected configuration from module one is used as the base point for further design iterations at fixed cruise altitude. The design is now optimized for low emissions with metrics ETS and ATR independently minimized. Modified wing and disk loadings are recorded as outputs for each measure.
4. The optimized wing and disk loading configuration from module three are used as base starting points to further minimize ETS and ATR as a function of cruise altitude.
5. The design in module four represents the optimum configuration (low emissions) in the formed framework. The emission performance of the optimum is evaluated against baseline by Silva et al. (Ref. 10) in module one.

The PSO algorithm is further used for objective function minimization when the problem scope is extended which limits the use of gradient-based methods. A variant of the original PSO method by Kennedy (Ref. 11) was developed by Khurana (Ref. 20) which incorporates adaptive mutation operators to induce search diversity, hence mitigate convergence to a local solution and was used in the analysis to follow. The algorithm has been extensively validated on benchmark test functions with demonstrated convergence to a global minima for complex solution topologies where input dimensionality size matches the scope of the rotorcraft sizing problem to follow. The algorithm has also been used with success for airfoil design problems (Ref. 14), and has been coupled with artificial neural networks to enhance the design computational time needed to derive efficient concepts in aerodynamic shape optimization applications (Ref. 21). Coupled with a parameter sensitivity study, the PSO runs are formulated to study the relationship between problem dimensionality and objective fitness so that total iterations needed to generate a solution remain low without compromising solution feasibility.

RESULTS

In the results to follow, a gradient-based process is first implemented to guide the solution toward an acceptable design point. The limitations with the applied approach are identified. To further progress the design phase, the PSO method is introduced and as pre-processing, design variable sensitivity methods are presented that quantitatively and qualitatively evaluate the degree-of-influence of the design variables on objective function. The results are then used to execute gradient-free optimization runs to establish a global optimum with minimal computational overhead.

Gradient-based analysis

Here, RCOTOOLS (Ref. 3) with OpenMDAO (Ref. 4) is used to generate data for the optimization cases outlined in Figure 1. The Sequential Least Squares Programming (SLSQP) method is applied to derive the gradients of the objective function. Optimization convergence is further assessed by the change in measurable output which needs to be within a user-defined tolerance over successive user-defined iterations.

- **Module One: Multi-Objective Optimization of Weights (fuel and empty) and Engine Power**
  The database of solutions generated by the sweep run are modeled in Figure 2.

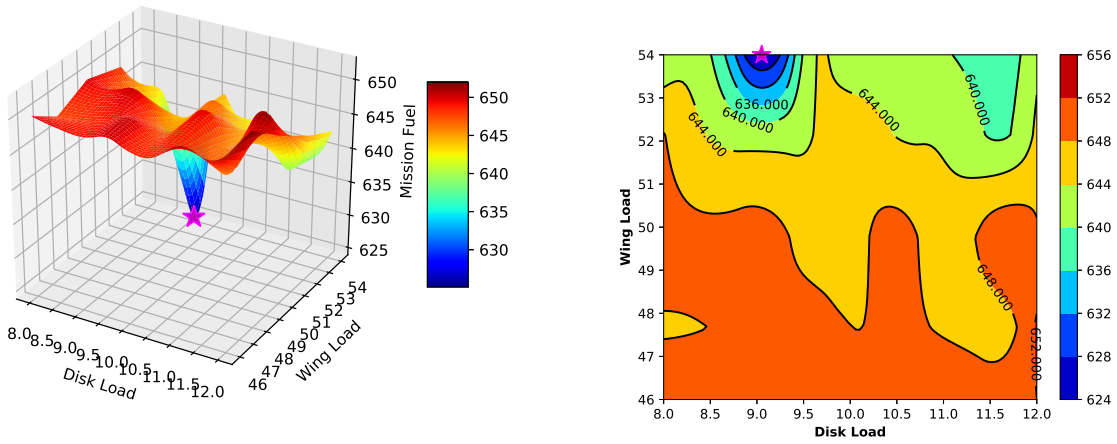

(a) 3-D surface representation

(b) 2-D contour representation

Fig. 2. Representation of the solution space as a function of wing and disk loadings on mission fuel weight at 25,000ft

The analysis confirms that the solution space for mission fuel weight is uneven and many sizing configurations exist for the defined objectives. This solution pattern is also consistent for empty weight and engine power. The solution topology is further sensitive to the magnitude of the weighting parameters and convergence at disparate configurations occurs for unique starting points. The multi-modality shown in this case is attributed to the interplay between aerodynamics, structures, propulsion, and emissions models. Studies involving a multi-disciplinary design optimization framework with the coupling of emission and acoustic models will refine the solution topology toward a global minima. Further stochastic methods will derive a solution toward a global point.

- **Module Two: Performance evaluation of baseline with Optimized Minima**
  The performances of the optimum platform from module one (symbol star in Fig. 2(a)) is evaluated against baseline (Ref. 10) in Table 2.

Table 2. Optimization for Low Weights and Engine Power Requirements at 25,000 ft

	WL	DL	W_{fuel} (lb)	W_{empty} (lb)	P_{req} (hp)	ETS (kg CO_2)	ATR (nano deg C)
Baseline (Ref. 10).	50.00	9.00	621.83	5535.51	798.58	1057.71	36.70
Optimum (Fig. 2)	54.00	9.63	624.75	5481.77	798.40	1062.68	36.70

Shaded entries represent decreased entries relative to baseline.

Relative to baseline, the optimum configuration from the parametric trade study resulted in a 0.50% increase in mission fuel weight; a 1.00% decrease in empty weight; with a negligible change in P_{req}. Emission metrics were not incorporated as objectives in this analysis, hence ETS increases by 0.50%, yet there is no change in ATR.

- **Module Three: Emission Optimization as a function of WL and DL at 25,000 ft**
  The optimum configuration from module one is further used to size WL and DL to independently minimize ETS and ATR. The converged configuration is evaluated against baseline in Table 3.

Table 3. Optimization for Low Emission at 25,000 ft

	WL	DL	W_{fuel} (lb)	W_{empty} (lb)	P_{req} (hp)	ETS (kg CO_2)	ATR (nano deg C)
Optimized Baseline (database in Module 2, Table 2)	54.00	9.63	624.75	5481.77	798.40	1062.68	36.70
Optimum for ETS	48.70	6.34	602.33	6132.30	800.00	1024.54	36.50
Optimum for ATR	54.25	6.00	604.67	6454.41	800.51	1028.52	36.40

Optimization for emission lowers mission fuel weight requirements relative to baseline with a reduction that is in excess of 3% for both ETS and ATR. As penalty, there is an increase in platform empty weight of the optimized designs at approximately 12% with the ETS-based design, and 18% with ATR. Engine power requirements only marginally increase with optimized configurations. Specifically as was the target, a decrease in emission is noted. The ETS generated solution has the objective reduced by almost 4% relative to baseline, and this further lowered ATR, which was not implemented in the objective function by approximately 0.50%. In the case of the ATR generated solution, the emission metric only decreases by 0.80% relative to initial configuration, and ETS reduction is limited to approximately 3% (recalling ETS was not included as objective in the ATR optimization run). The results confirm that a design compromise will be required to balance acceptable emission performances with empty weight.

- **Module Four: Emission Optimization as a function of Cruise Altitude**
  The converged WL and DL configurations from module three for low ETS and ATR performances at 25,000 ft are fixed and are now used to optimize cruise altitude in an effort to further lower emissions.

Table 4. Cruise altitude optimization for Low Emissions

	WL	DL	W_{fuel} (lb)	W_{empty} (lb)	P_{req} (hp)	ETS (kg CO_2)	ATR (nano deg C)
ETS @ 25,000 ft	48.70	6.34	602.33	6132.30	800.00	1024.54	36.50
ETS @ 26,250 ft	48.70	6.34	601.35	6131.29	800.00	1022.89	54.30
ATR @ 25,000 ft	54.25	6.00	604.67	6454.41	800.51	1028.52	36.40
ATR @ 20,000 ft	54.25	6.00	610.22	6432.42	772.24	1040.30	6.73

The optimized altitude for ETS minimization increases by 1,250 ft to 26,250 ft from baseline setting. This has the impact of marginally lowering W_{fuel} and W_{empty} with no change to P_{req}. ETS is also marginally lowered, yet due to cruise at higher altitude, ATR increases significantly by approximately 49%.

In the study of optimizing ATR, the best cruise altitude is lowered from 25,000 ft to 20,000 ft. Accordingly there is an increase in W_{fuel} by almost 1%; W_{empty} lowers slightly; and P_{req} decreases by approximately 3.50%. A cruise at lower altitude adversely impacts ETS which has an increase in excess of 1%, yet ATR is lowered significantly by almost 82% as was the objective.

- **Module Five: Emissions Performance Evaluation against Baseline**
  As summary, the emissions at the optimized WL, DL and cruise altitudes are evaluated against baseline (Ref. 10) to quantify the performance improvements by optimization.

Table 5. Evaluation of emissions performance of optimized concepts with baseline

	WL	DL	W_{fuel} (lb)	W_{empty} (lb)	P_{req} (hp)	ETS (kg CO_2)	ATR (nano deg C)
Baseline @ 25,000 ft	50.00	9.00	621.83	5535.51	798.58	**1057.71**	**36.70**
ETS @ 26,250 ft	48.70	6.34	601.35	6131.29	800.00	1022.89	54.30
ATR @ 20,000 ft	54.25	6.00	610.22	6432.42	772.24	1040.30	6.73

Shaded entries represent decreased emission relative to baseline (in bold).

In comparison to baseline, optimized concepts are configured with low DL which significantly increases W_{empty}, yet the magnitude of W_{fuel} decrease is marginal in comparison. There is a negligible change in P_{req} at higher altitudes as baseline and ETS optimized configurations are operating within a 1,250 ft range of one another. The increase in cruise altitude with an ETS focus design lowers ETS by approximately 3% relative to baseline, yet there is a significant increase in ATR by almost 50%.

The ATR generated concept which is cruising at a lower altitude relative to baseline is requiring a slight increase in fuel demands, and the low DL is attributing to a higher W_{empty}. Low altitude operation is further attributing to a decrease in P_{req}. From an emissions perspective, ETS is decreased by 1.64% and the most significant decrease is with ATR that is lowered by almost 82%.

The gradient-based optimization module adopted in the works (Fig. 1) is not ideal as it consists of many steps (studies) which need to be carefully defined to iteratively refine the search space, hence guide the solution toward low emission flight. The analysis further confirmed that a multi-modal solution space exists, hence population-based optimization methods are considered. Evolutionary Algorithms (EA) which are inspired by biological evolution do not require a starting point to the design problem, and the search also does not rely on the computation of objective gradients, hence are ideal to address the observed limitations with the gradient design approach.

Design Variable Sensitivity Analysis using qualitative means

To facilitate optimization using population based algorithms, the sensitivity of the input parameters on output is assessed so that variables that have minimal influence on objectives are identified. The qualitative representation of parameter sensitivity on objective function is first assessed using a full factorial plan. A test matrix of rotorcraft configurations are formed by combinations of pairwise permutations of k sizing variables. The parameters are perturbed two-way over p levels with the remaining variables held constant at their respective baseline setting. For each pairwise interaction, emission is established using NDARC and the data is projected using contour plots. An estimate of the interaction effects is then visually established to extract the underlying patterns or features that exists in the data.

In this framework, additional design variables are introduced in Table 6 together with WL and DL parameters from earlier gradient-based runs to progress the conceptual sizing effort using evolutionary methods. Parameter intervals are mapped to represent the optimization search space envelope, and the input-to-output sensitivity is assessed in this range. The baseline configuration by Silva et al. (Ref. 10) is also presented for reference.

Table 6. HECTR baseline design parameters with interval ranges used for sensitivity analysis on emissions

	f_{cd}	$VTIP_{REF(1)}$	DL	WL	f_{span}	$thickTR$	$tSpan$	Alt.	$Vtip$
Baseline (Ref. 10)	0.00352	750	9	50	0.05	0.20	15	25k	383
Intervals	[0.00332,0.00435]	[730,763]	[6,11]	[45,56]	[0.05,0.19]	[0.18,0.23]	[11,19]	[12k,26.5k]	[340,480]

Where: DL = Disk Loading; WL = Wing Loading; f_{cd} = Fuselage drag coefficient; f_{span} = ratio of wing panel span to wing span (one side); $tSpan$ = Tail Span; $thickTR$ = tiltrotor wing airfoil thickness-to-chord ratio; $VTIP_{REF(1)}$ = Main rotor tip Velocity at hover = 70% of tip velocity of tail rotor $VTIP_{REF(2)}$; Altitude (ft) = Segment 4 (Table 1); and $Vtip$ = Mission segment 4 tip velocity as a fraction of tip velocity at hover.

Each of the $k = 9$ design parameters in Table 6 are permutated with $p = 6$ levels across the defined interval range. The objective function is sampled on a $p \times p$ full factorial plan which corresponds to the projection of input-to-output data on $\frac{k(k-1)}{2} = 36$ contour tiles. This results in a database of 1296 points (sample size in each tile $\times$ number of tiles = 36×36) which are qualitatively presented in Figures 3 and 4 for ETS and ATR respectively.

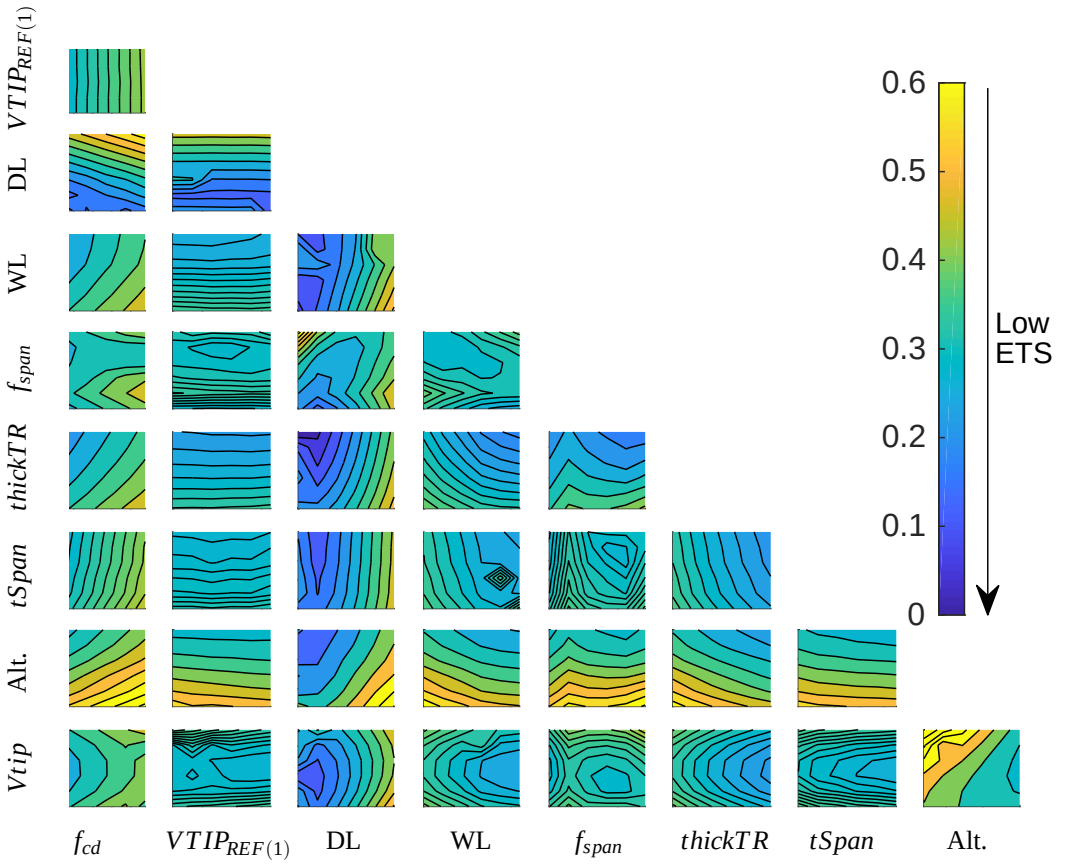

Fig. 3. Pair-wise interaction of sizing variables on ETS (Kg CO_2); contours normalized to range [0.0,1.0]; for clarity, maximum contour level is fixed to 0.60

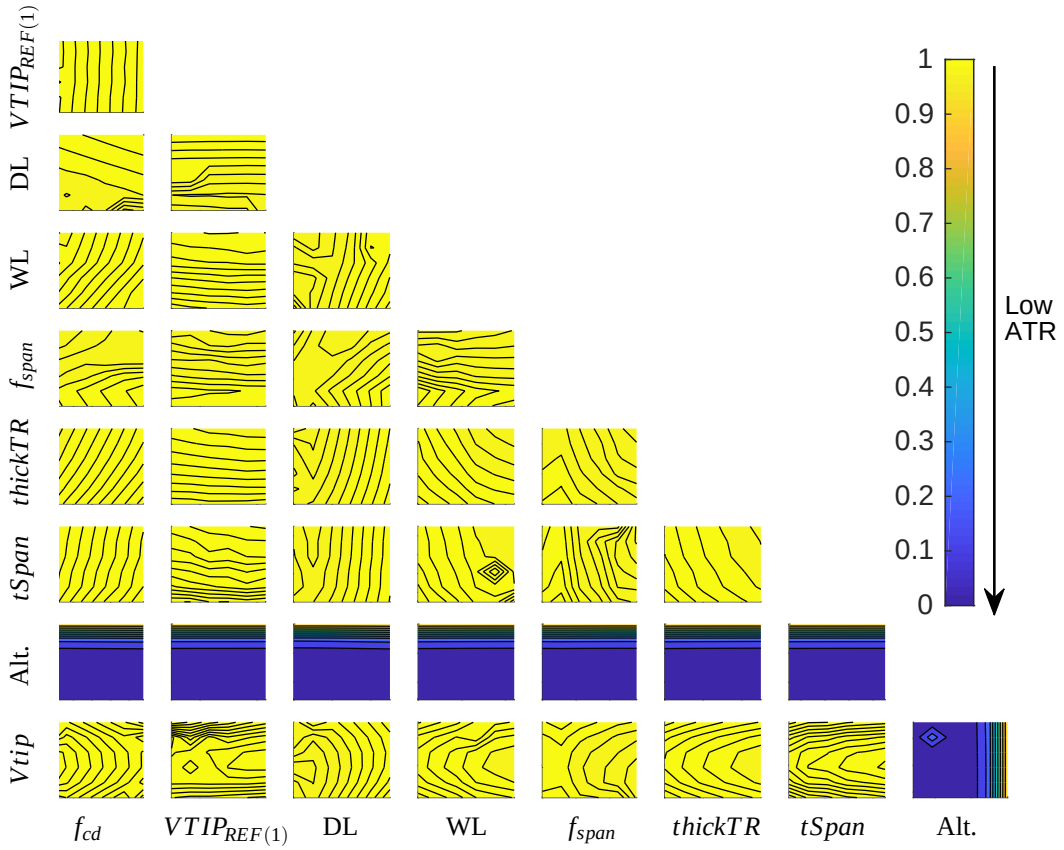

Fig. 4. Pair-wise interaction of sizing variables on ATR (nano deg C); contours normalized to range [0.0,1.0]

The x and y axis on each tile represent the design variable limits from Table 6 and the normalized contours model the output magnitude. Figure 3 confirms that the design variables collectively influence ETS and distinct patterns have emerged. For instance, low DL readings correspond to low ETS and this activity persists across all design parameters. As was to be expected, low altitude flight increases emissions, hence low altitude cruise is to be avoided. The highest ETS value recorded in the database was with variation in altitude and fraction of cruise tip velocity to tip velocity at hover (top left corner of Alt. vs. $Vtip$ tile). These parameters will have a significant influence toward achieving low ETS flight in gradient-free optimization runs to follow.

Relatively, the evolution of ATR with pair-wise variations of the sizing parameters confirms a stagnant pattern in Figure 4. Here, altitude alone is shown to impact the output metric. Specifically low altitude flight favorably results in low ATR performances and this pattern is directly opposite to the high ETS performances that were modeled in Figure 3 at low altitudes. Theoretically, ATR quantifies the lifetime global mean temperature change caused by operation of an aircraft, as a measure of climate change (Ref. 22). The metric is a function of radiative forcing (RF) which is an instantaneous measure that quantifies the change in energy that produces changes in climate properties. The total RF that is generated by pollutants CO_2, NO_x, and Aviation Induced Cloudiness (AIC) is used to calculate the global temperature response that further factors the operating lifetime of the aircraft to determine the total climate impact.

AIC further factors contrails and aviation-induced cirrus clouds, hence is a function of cruise altitude (Ref. 22). Design for minimum ATR factors the time horizon, discount rate, operating altitude and speed, including engine technology. If long-term effects are not considered, then radiative forcing due to CO_2 influences ATR with high cruise altitude. If only short-term impacts are factored, then NO_x emissions have a greater impact, and a lower cruise altitude results in decreased climate impact, despite increased fuel burn and CO_2 emissions. The inclusion of AIC in the analysis of ATR has a significant impact on the design, and a low cruise altitude is preferred. This pattern was qualitatively captured in Figure 4.

In the optimization problems to follow, minimization of ETS will be the focus as there are active interactions between the nine variables on objective (Fig. 3). Relatively in the analysis for ATR, only altitude was an influencing factor (Fig. 4). Accordingly ETS minimization is well suited for analysis by a stochastic method.

Design Variable Sensitivity Analysis using quantitative means

The qualitative plots in Figures 3 and 4 do not provide a statistical measure of the sensitivities between model inputs and outputs, and a quantitative approach is needed to establish these measures. Morris screening algorithm (Ref. 23) is used and applies a Design of Experiment (DoE) approach to perturb the design variables one-factor-at-a-time to form a relationship between inputs and model output. A detailed mathematical derivation and execution of the Morris sensitivity method is documented in the literature (Refs. 14, 24–29). Here the procedure is briefly outlined:

1. The method is initiated by selecting a base trajectory of randomised values, $\boldsymbol{X}^*$, of all respective input variables, $\boldsymbol{X}$, such that they are in the defined ranges of set values. The subsequent model output is established.

2. Change the value of one randomly selected variable in the i^{th} component of trajectory $\boldsymbol{X}^*$ by $\pm\Delta$ such that the perturbed vector $\boldsymbol{X}^{(1)}$ is still in the defined variable limits. The other inputs maintain their respective start values. Model output of $\boldsymbol{X}^{(1)}$ is established.

3. Value of another sampling point $\boldsymbol{X}^{(2)}$ is modified $\pm\Delta$ with previous modified variable $\boldsymbol{X}^{(1)}$ held at its changed value, and all other factors at their original start values. Hence, a constraint on $\boldsymbol{X}^{(2)}$ requires that it differs from $\boldsymbol{X}^{(1)}$ in the randomly selected i^{th} component by $\pm\Delta$. The model output is again established following $\boldsymbol{X}^{(2)}$ perturbation.

4. Hence, from above the method requires that each point in trajectory $\boldsymbol{X}^*$ differs from the preceding one by only one coordinate. Variable modification steps are repeated for all input factors, hence in a trajectory each input parameter only changes once by a predefined step $\pm\Delta$, and at each perturbation, model output is established.

5. Repeat steps 1–4 $r-$ times and, at each run, a different vector of start values (trajectories) $\boldsymbol{X}^*$ is set to ensure an acceptable coverage of design points in the parameter space is factored for sensitivity evaluation.

The trajectories from $r-$runs are then used to evaluate the coefficient of variation (sensitivity) by the measure of the elementary effect (EE) of each input variable, i, on model output. The EE is computed between two points of the trajectory using:

$$EE_i(\boldsymbol{X}) = \frac{Y(\boldsymbol{X} + \Delta e_i) - Y(\boldsymbol{X})}{\Delta}. \tag{3}$$

Where the divisor Δ is a user-defined fixed step size, and e_i is the i^{th} unit vector. Hence, each EE was computed with observations at the pair of points $\boldsymbol{X}$ and $\boldsymbol{X}+\Delta e_i$.

A set of r different random trajectories (index R) is defined in the hypercube of input variables, which provides r estimates of EE_{iR} for each input variable i. With this, there are $r(k+1)$ evaluations of the model output, Y. The mean, μ, and standard deviation, σ, of the EE is computed for each input variable i by:

$$\mu_i = \frac{1}{r}\sum_{R=1}^{r} EE_i(\boldsymbol{X}_R) \tag{4}$$

and

$$\sigma_i = \sqrt{\frac{1}{(r-1)}\sum_{R=1}^{r}[EE_i(\boldsymbol{X}_R)-\mu_i]^2}. \tag{5}$$

A modification of measure μ was proposed by Campolongo et al. (Ref. 30) with μ_i^*, which uses the distribution of the absolute values of EE in Equation 6. If the distribution of the EE contains a negative element, which occurs when the model is non-monotonic, some effects may cancel each other out when computing the mean. This will not provide a reliable measure of the ranking of the importance of design factors (variables) on model output. Instead, it is suggested that the mean should only be computed on the absolute values of EE with μ_i^* so that the occurrence of the effects of opposite signs is avoided.

$$\mu_i^* = \frac{1}{r}\sum_{R=1}^{r} |EE_i(\boldsymbol{X}_R)|. \tag{6}$$

Even with μ_i^*, the standard deviation (Eqn. 5) of EE remains a critical indicator of the non-linearity in input parameters on model output by interaction with other state variables. By plotting the two statistical measures, the Morris method classifies input i to have the following effect on model output:

1. **Negligible:** Low mean and low standard deviation.
2. **Linear and additive:** High mean and low standard deviation.
3. **Non-linear or involved in interactions with other input parameters:** High standard deviation.

In this analysis, $r = 200$, random trajectories of the input variables were modeled, hence $r(k+1) = 200(9+1) = 2000$ rotorcraft configurations were formed for variable screening. In Figure 5, the sensitivity distribution of the inputs from Table 6 on ETS are ranked as the summation of μ_i^* and σ.

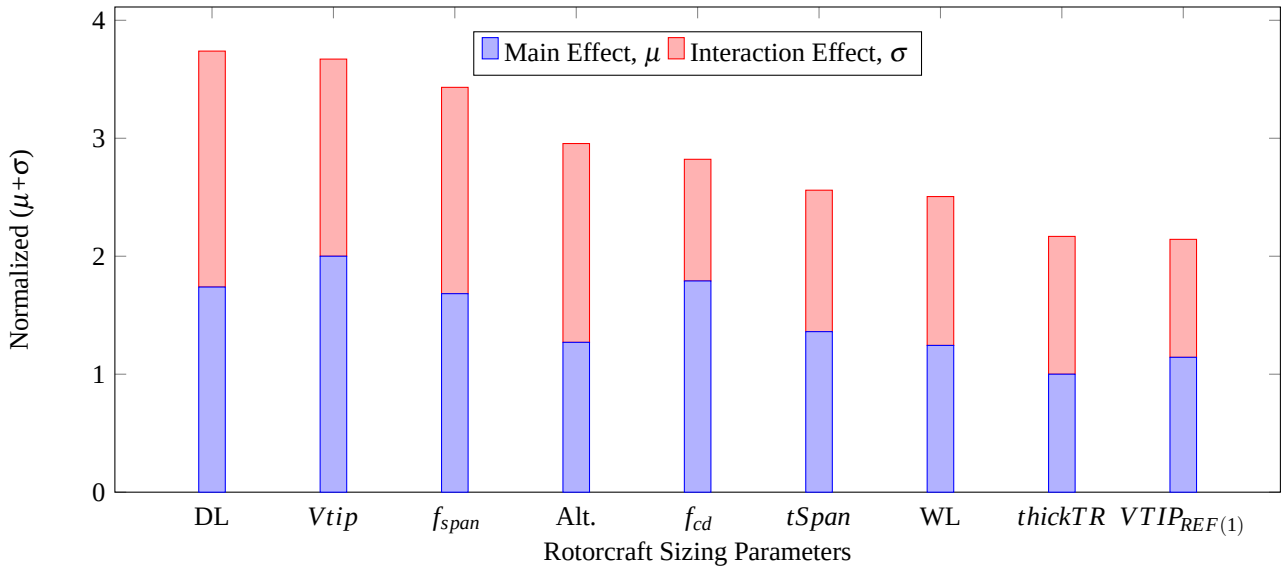

Fig. 5. Ranking of main first order and interaction effects of rotorcraft sizing parameters on ETS

In Figure 5, DL is ranked as the highest contributing factor to ETS by the summation of the main and collective interaction effects with other parameters. Variable $Vtip$ follows with the level-of-importance that closely matches that of DL. At the other end of the spectrum, $VTIP_{REF(1)}$ is established with the lowest impact, even though the main effect is not the lowest recorded, yet it does have minimal interaction relative to other parameters in influencing the objective measure. The knowledge gained from this analysis will guide the formation of optimization runs using gradient-free methods.

Optimization using the Particle Swarm Theory

The limitations of the gradient-based optimization method to establish a near optimum solution for a simplified two-dimensional sizing case with DL and WL as input parameters has been established. This challenge is now addressed with the PSO method (Ref. 20) that is capable of handling a greater degree-of-dimensionality as optimization inputs without compromising global optimality. The data from the design variable sensitivity analysis using the quantitative approach in Figure 5 provides critical information that is used to define the dimensionality of the problem. Specifically optimization runs to be executed from the perspective of input dimensionality include: **(a)** *full set* of nine input parameters; and **(b)** *reduced set* with the removal of unimportant parameter(s) identified in Figure 5. The analysis will confirm the impact of input dimensionality on optimality and on convergence rate.

An unconstrained optimization framework is formed with the objective function defined to minimize ETS. The limits of the design variables from Table 6 are used and the PSO algorithm is further setup as follows:

(a) A swarm size of 20 particles.

(b) The maximum velocity of the particles was capped as a function of variable dimensional search space. This setting controls the scalar step length, α, or the maximum size of the variable rate-of-change at each iteration. Numerical experiments are performed to establish the magnitude of α.

(c) To mitigate convergence to a local minima, mutation operators were activated based on the principles developed by Khurana and Massey (Ref. 20). Probability of mutation is governed by the search patterns of the particles that is dynamically monitored during the iterative cycle. The adaptive process ensures that mutation is most active when the swarm is converging to a solution region so that a local minima is avoided.

(d) Optimization termination is set when the fitness of the global best particle; personal best fitness of the worst performing particle in the swarm subtracted from the fitness of the global best; and the standard deviation of the personal best fitness of each particle in the swarm collectively do not change over five successive iterations. This approach was previously validated by Khurana and Massey (Ref. 20)

In the PSO run with a *reduced set* analysis, $VTIP_{REF(1)}$ was not factored in the optimization (was set at default baseline value), hence the dimensionality of the optimization was limited from nine variables (*full set*) to eight. The converged fitness with iterations needed to achieve an optimum configuration for low ETS performance is presented in Figure 6.

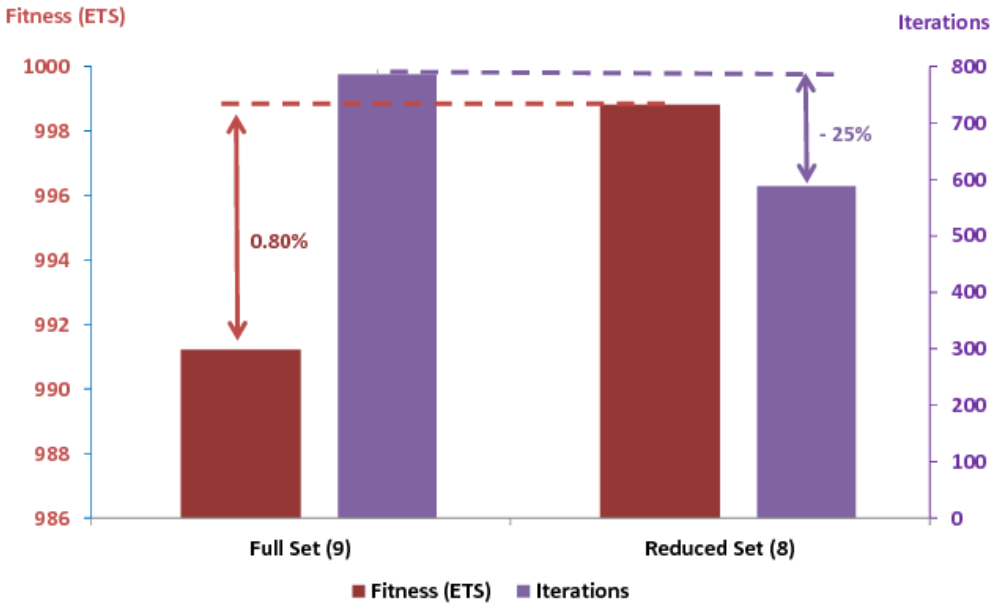

Fig. 6. PSO fitness and convergence iterations results with nine variables versus eight

To establish an acceptable magnitude of particle scalar step length, α, several PSO runs were executed and the converged ETS result was noted. The solutions were within a 1% variance and the setting with the lowest ETS was with a step length of 75% of dimensional search space in Figure 6. The analysis reinforced that PSO results are not sensitive to starting points as in gradient-free methods since the search volume is randomly populated and a negligible change in model output was established across the independent optimization runs.

Figure 6 further validates a reduction in input dimensionality has a minimal impact on converged ETS and significant on iterations needed to achieve a solution. As is shown, ETS is higher with reduced variable set relative to full population of parameters with a difference that is less than 1%. Yet, the reduced set significantly lowers the number of PSO iterations that are needed for convergence. A 25% reduction results in several hours of computing time saving relative to the full set. This is significant even when NDARC, as a low-fidelity solver is used in the analysis. This computational benefit will be transferable when higher fidelity solvers are used in the optimization loop at detail design.

The result is further interpreted to establish whether there is an acceptable balance between solution feasibility and computational efficiency. A 0.80% difference in solution optimality appears minimal, yet it is critical that platform configuration is not compromised at conceptual design to ensure design improvements follow at detail design. A significant reduction in computing overheads is noted with reduction in problem dimensionality, yet at conceptual sizing this benefit does not outweigh a compromised solution. The knowledge gained from the sensitivity analysis and optimization runs will be applicable in detail design iterations where higher fidelity solvers are used, and changes to platform configuration required to sustain further performance improvements can be localized to critical sizing parameters that have been identified through this analysis. Hence, at conceptual design where low fidelity solvers are used and computational overhead is minimal, it is justified that all parameters-of-interest are included in the sizing to ensure optimality is not compromised.

As comparison, the performances of the configurations formed in the analysis are summarized in Table 7

Table 7. Comparative analysis of the established rotorcraft configurations using optimization methods relative to baseline

	f_{cd}	$VTIP_{REF(1)}$	DL	WL	f_{span}	$thickTR$	$tSpan$	Alt.	$Vtip$	ETS (kg CO_2)
Baseline (Ref. 10)	0.00352	750	9.00	50.00	0.050	0.20	15.00	25,000	383	1057.71
Gradient-Based (Module 4 - Tab. 4)	0.00352	750	6.34	48.70	0.050	0.20	15.00	26,250	383	1022.89
PSO (Full Set - Fig. 6)	0.00365	731	6.52	51.18	0.053	0.22	18.50	23,565	395	991.22
PSO (Reduced Set - Fig. 6)	0.00340	750†	6.07	51.18	0.056	0.23	18.37	23,016	409	998.81

Shaded entry represents minima ETS performance.
† Baseline value.

The optimization data using both gradient-based and gradient-free methods in Table 7 result in performance improvements relative to baseline. The gradient optimization process lowers ETS by $\approx 3\%$ with the manipulation of DL, WL, and cruise altitude following the optimization modules outlined in Figure 1. Here, DL and WL are lowered, and cruise altitude is increased relative to baseline to sustain the noted performance improvement. The PSO simulations model an extended design space envelope in an effort to further improve ETS performance. Both full and reduced variable set simulations result in ETS performance enhancements relative to the gradient-based optimization analysis. The full set PSO study lowers ETS by an additional $\approx 3\%$ than the best solution generated by the gradient-optimization method, and the reduced variable set has a performance improvement that is $\approx 2\%$ lower. The performance gains between the two PSO runs is limited to $< 1.0\%$, but are significantly higher than baseline.

The convergence of the full set PSO sizing parameters yields solutions that warrants further analysis to ensure global optimality has been achieved. Considering f_{cd}, there is scope for additional enhancements to ETS especially if it is assumed that airframe improvements with streamlined designs will lower drag, hence minimize fuel burn. The converged f_{cd} is higher than baseline and gradient-optimization result even though the interval for f_{cd} (Tab. 6) facilitates search at lower drag performances. The result suggests that the low drag region was not exploited by the PSO to sustain maximum available improvements.

Altitude is another parameter which is assumed to be at a non-converged state in the two PSO runs from a global optimality perspective. Recalling in Figure 3, it was qualitatively shown that high altitude performances lower ETS, but in the PSO full set converged state the cruise altitude is low at 23,565 ft in comparison to 25,000 ft for baseline and 26,250 for the gradient-based result. The upper limit of the altitude interval range in Table 6 that is available for the PSO to exploit is set at 26,500 ft. Yet the converged result is at a lower setting and directly contradicts with the expected performance gains that are achievable based on the data from the sensitivity analysis in Figure 3.

Considering the convergence of other parameters that have contributed to the lowering of ETS relative to the gradient-based and baseline include increases in platform WL; f_{span}; $thickTR$; $tSpan$; and $Vtip$. This pattern is further consistent in

the PSO run with reduced variables where $VTIP_{REF(1)}$ was set at baseline. Further in the reduced variable set analysis, even though the converged f_{cd} is at the minimum state, it is still not at the lowest setting that is available for exploration by the PSO ($cd_{min} = 0.000332$ in Tab. 6). With this, further design improvements are likely. Similar to the full set PSO run, cruise altitude is also converged at a low setting and higher altitudes will increase ETS performance. The coupling of f_{cd} and altitude alone will drive improvements that will reduce the ETS performance gap between the two PSO runs in Figure 6 to a negligible difference.

In future works, the integration of a gradient-based optimization algorithm as a post-processor to a converged PSO solution is a viable path forward in an effort to address the above points. In this approach, the swarm algorithm is first used to navigate the search toward a solution region bounded about the global minima, and in the process will bypass the local valleys that exist in the search volume (as was confirmed in Figure 2). Once at the global region, local search patterns need to be activated. Here, the input from the converged PSO solution can be used as the initialization point for a gradient-based analysis to guide the solution, using a suitable scalar step length, to a global minima. Specifically the issues relating to the non-convergence of f_{cd} and altitude, and possibly other parameters will be addressed.

The inclusion of ATR, including platform weights (empty and fuel) as objectives in PSO also needs to be considered. The data visualization charts in Figures 3 and 4 showed that altitude variations have an opposing impact on ETS and ATR. Further, single objective optimization focused on ATR minimization was not justified as altitude alone was determined to be an influencing parameter. Yet, ATR minimization needs to be considered in the sizing and a multi-objective optimization formulation is required that further factors ETS with ATR and platform weights. A design compromise that yields acceptable performances between emissions and weights can then be established.

CONCLUSION

A computational framework encompassing design optimization tools for rotorcraft conceptual sizing was presented. A gradient-based optimization approach was first applied to improve emission performance of the baseline with the optimization of platform WL and DL. The analysis confirmed that a multi-modal solution space exists, hence local optima solutions were established. A population-based stochastic algorithm based on the particle swarm theory was then used to address this shortfall. A design variable sensitivity analysis was undertaken to qualitatively and quantitatively model the influence of rotorcraft sizing parameters on emissions. It was shown that DL had a significant impact on ETS, while the tip velocity at hover for the main rotor had minimal influence. Two PSO runs were then formed that: **(a)** encompassed all sizing parameters; and **(b)** with reduced dimensionality to evaluate the relative impact of problem definition on solution feasibility and computational efficiency. The objective from the two PSO runs were within 1%, yet the reduced dimensionality case converged with 25% fewer iterations. Examination into the state of the PSO established solutions suggests that a global optima has still not been achieved and the utilization of gradient-based tools, as a post-processor to the swarm solution is a justifiable next step.

The concepts presented are developed to aid rotorcraft conceptual sizing where the knowledge gained from the analysis can be applied in detail design. Population based optimization methods are not suited when input dimensionality is extreme coupled with high fidelity solvers as the computational overheads, even with parallel computing will be extreme. The results to the sensitivity analysis are transferable for use at detail designs where variable(s) that have a significant impact on the objective measure can be targeted to exploit for further performance gains. Gradient-based tools are important at conceptual design to identify the topology of the solution landscape. These methods will also be critical in detail designs to further fine-tune the solution since a well-defined starting point will exist as output to an evolutionary search process from the conceptual design phase.

ACKNOWLEDGMENTS

The authors acknowledge Larry A. Meyn, NASA Ames Research Center, for his technical support in the setup and execution of RCOTOOLS.

REFERENCES

[1]Nicolas E. Antoine and Ilan M. Kroo. Framework for aircraft conceptual design and environmental performance studies. *AIAA Journal*, 43(10):2100–2109, 2005.

[2]Wayne Johnson. NDARC - NASA design and analysis of rotorcraft. NASA/TP 2015-218751, NASA Ames Research Center, Moffett Field, CA United States, 2015.

[3]Larry A. Meyn. Rotorcraft optimization tools: Incorporating rotorcraft design codes into multi-disciplinary design, analysis, and optimization. In *Specialists Conference on Aeromechanics Design for Transformative Vertical Flight*, January 2018.

[4]K. Moore, B. Naylor, and Justin S. Gray. The development of an open-source framework for multidisciplinary analysis and optimization. In *Proceedings of the 10th AIAA/ISSMO Muldisiciplinary Analysis and Optimization Conference*, August 2008.

[5]Wayne Johnson and Jeffrey D. Sinsay. Rotorcraft conceptual design environment. In *The 2nd International Forum on Rotorcraft Multidisciplinary Technology*, October 2009.

[6]Max Lier, Alex Krenik, Philipp Kunze, Dieter Kohlgrber, Marius Ltzenburger, and Dominik Schwinn. A toolbox for rotorcraft preliminary design. In *AHS 71st Annual Forum*, May 2015.

[7]J. Enconniere, J. Ortiz-Carretero, and V. Pachidis. Mission optimisation for a conceptual coaxial rotorcraft for taxi applications. *Aerospace Science and Technology*, 72:1–15, 2017.

[8]F. Ali, I. Goulos, and V. Pachidis. An integrated methodology to assess the operational and environmental performance of a conceptual regenerative helicopter. *The Aeronautical Journal*, 119(1211):67–90, 2015.

[9]Carl Russel and Pierre-Marie Basset. Conceptual design of environmentally friendly rotorcraft a comparison of nasa and onera approaches. In *AHS 71st Annual Forum*, May 2015.

[10]Christopher Silva, Wayne Johnson, and Eduardo Solis. Multidisciplinary conceptual design for reduced-emission rotorcraft. In *Specialists Conference on Aeromechanics Design for Transformative Vertical Flight*, January 2018.

[11]J. Kennedy and R. Eberhart. Particle swarm optimization. In *Neural Networks, 1995. Proceedings., IEEE International Conference on*, volume 4, pages 1942–1948 vol.4, Nov 1995.

[12]Manas Khurana, Hadi Winarto, and Arvind Sinha. Application of swarm approach and artificial neural networks for airfoil shape optimization. In *12th AIAA/ISSMO Multidisciplinary Analysis and Optimisation, Victoria, British Columbia, Canada*, 2008.

[13]Manas Khurana, Hadi Winarto, and Arvind Sinha. Airfoil optimisation by swarm algorithm with mutation and artificial neural networks. In *47th AIAA Aerospace Sciences Meeting, Victoria, Orlando, USA*, 2009.

[14]Manas Khurana and Hadi Winarto. Development and validation of an efficient direct numerical optimisation approach for aerofoil shape design. *The Aeronautical Journal*, 114:611–628, 2010.

[15]Jeffrey M. Badyrka, Roy J. Hartfield, and Rhonald M. Jenkins. Aerospace design optimization using a compound repulsive particle swarm. *Applied Mathematics and Computation*, 219(15):8311 – 8331, 2013.

[16]T. D. Chollom, N. Ofodile, and O. Ubadike. Application techniques of multi-objective particle swarm optimization: Aircraft flight control. In *2016 UKACC 11th International Conference on Control (CONTROL)*, pages 1–6, Aug 2016.

[17]Chen chao Xia, Ting ting Jiang, and Wei fang Chen. Particle swarm optimization of aerodynamic shapes with nonuniform shape parameter–based radial basis function. *Journal of Aerospace Engineering*, 30(3):04016089, 2017.

[18]Qi Bian, Xinmin Wang, Rong Xie, Ting Li, and Tianli Ma. Small scale helicopter system identification based on modified particle swarm optimization. In *2016 IEEE Chinese Guidance, Navigation and Control Conference (CGNCC)*, pages 182–186, Aug 2016.

[19]Adriana Andreeva-Mori, Keiji Kobayashi, and Masato Shindo. Swarm algorithm with adaptive mutation for airfoil aerodynamic design. *JOURNAL OF AEROSPACE INFORMATION SYSTEMS*, 12(10):646–659, 2015.

[20]Manas Khurana and Kevin Massey. Swarm algorithm with adaptive mutation for airfoil aerodynamic design. *Swarm and Evolutionary Computation*, 20:1–13, 2014.

[21]Manas Khurana. *Development and Application of an Optimisation Architecture with Adaptive Swarm Algorithm for Airfoil Aerodynamic Design*. PhD thesis, School of Aerospace, Mechanical and Manufacturing Engineering, RMIT University, Melbourne, Australia, 2011.

[22]Wayne Johnson. NDARC NASA design and analysis of rotorcraft theory. NASA Technical Report Release 1.11, 2016.

[23]M.D. Morris. Factorial sampling plans for preliminary computational experiments. *Technometrics*, 33:161–174, 1991.

[24]Che sheng Zhan, Xiao meng Song, Jun Xia, and Charles Tong. An efficient integrated approach for global sensitivity analysis of hydrological model parameters. *Environmental Modelling & Software*, 41(0):39 – 52, 2013.

[25]David Garcia Sanchez, Bruno Lacarrière, Marjorie Musy, and Bernard Bourges. Application of sensitivity. *CoRR*, abs/1203.3055, 2012.

[26]Hugo Maruri-A, Alexis Boukouvalas, and John Paul Gosling. Sequential screening with elementary effects. Oral presentation, School of Mathematical Sciences, Queen Mary, University of London, United Kingdom, 2011.

[27]Thomas Sumner. *Sensitivity Analysis in Systems Biology Modelling and its Application to a Multi-Scale Model of Blood Glucose Homeostasis*. PhD thesis, Centre for Mathematics and Physics in the Life Sciences and Experimental Biology, University College, London, United Kingdom, 2010.

[28]Haruko M. Wainwright, Stefan Finsterle, Yoojin Jung, Quanlin Zhou, and Jens T. Birkholzer. Making sense of global sensitivity analyses. *Computers & Geosciences*, 65:84–94, April, 2014.

[29]F. Campolongo A. Saltelli, S. Tarantola and M. Ratto. *Sensitivity Analysis in Practice*. John Wiley & Sons, Ltd, Ispra, Italy, 2004.

[30]J. Carboni F. Campolongo and A. Saltelli. An effective screening design for sensitivity analysis of large models. *Environmental Modelling & Software*, 22:1509–1518, 2007.